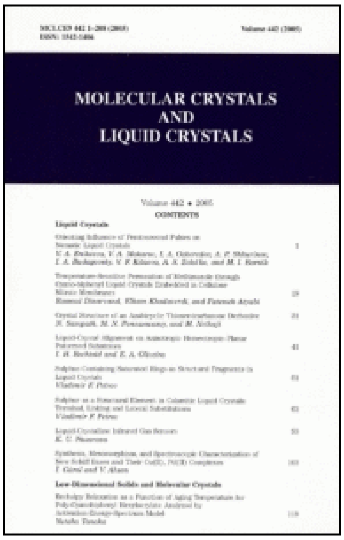

Molecular Crystals and Liquid Crystals
Publication details, including instructions for authors and subscription information:
http://www.informaworld.com/smpp/title~content=t713644168

Synthesis and Mesomorphic Properties of Tolane-Based Fluorinated Liquid Crystals with an Acrylate Linkage

Ximin Chen[a]; Yuehai Shen[b]; Jianxun Wen[a]
[a] Shanghai Institute of Organic Chemistry, Chinese Academy of Sciences, Shanghai, China [b] Faculty of Life Sciences and Technology, Kunming University of Science and Technology, Kunming, China

To cite this Article Chen, Ximin , Shen, Yuehai and Wen, Jianxun(2010) 'Synthesis and Mesomorphic Properties of Tolane-Based Fluorinated Liquid Crystals with an Acrylate Linkage', Molecular Crystals and Liquid Crystals, 528: 1, 138 — 146
To link to this Article: DOI: 10.1080/15421406.2010.504638
URL: http://dx.doi.org/10.1080/15421406.2010.504638

Mol. Cryst. Liq. Cryst., Vol. 528: pp. 138–146, 2010
Copyright © Taylor & Francis Group, LLC
ISSN: 1542-1406 print/1563-5287 online
DOI: 10.1080/15421406.2010.504638

Synthesis and Mesomorphic Properties of Tolane-Based Fluorinated Liquid Crystals with an Acrylate Linkage

XIMIN CHEN,[1] YUEHAI SHEN,[2]
AND JIANXUN WEN[1]

[1]Shanghai Institute of Organic Chemistry, Chinese Academy of Sciences, Shanghai, China
[2]Faculty of Life Sciences and Technology, Kunming University of Science and Technology, Kunming, China

Six series of tolane-based fluorinated liquid crystals containing an acrylate linker were synthesized and their mesomorphic properties were characterized. The compounds generally exhibit SmA and N phases in wide temperature ranges. The introduction of acrylate linkers increases the clearing points by 20°C–30°C and suppresses the formation of higher ordered monotropic SmB phases. para-*Fluorination is favorable for the mesophase stability, whereas* meta-*fluorination is not. The introduction of a 2,3,5,6-tetrafluorophenylene group decreases the clearing points and also suppresses the formation of the monotropic SmB phase.*

Keywords Cinnamate; fluorine; liquid crystals; tolane

Introduction

Because of their unique polar and steric effects, fluorine substituents in liquid crystals (LCs) often bring desirable changes in respect to melting point, mesophase morphology, transition temperatures, thermal stability, and essential physical properties such as optical and dielectric anisotropy [1–5]. Tolane-based fluorinated LCs are useful electro-optic media with low viscosity and high birefringence and thus have attracted considerable attention recently [6–8]. Study along this line has covered many three- and four-ring systems; for example, bistolane [9], biphenyltolane [10,11], biphenyl bistolane [12], tolane benzoate [13,14], and tolane cyclohexanylbenzoate [15].

Compared with an acetylene or an ester linker, an acrylic ester bridge [(*E*)−CH=CH−COO−] in a rod-like LC molecule extends the conjugated system and is likely to result in a higher clearing point. Liquid-crystalline cinnamate photopolymers are also used in making orientation films of liquid-crystal displays (LCDs) [16]. Therefore, we designed a three-ring system containing fluorinated cinnamate

---

Address correspondence to Yuehai Shen, Faculty of Life Sciences and Technology, Kunming University of Science and Technology, 296 Bailong Si, Kunming 650216, China. E-mail: yuehaishen@gmail.com

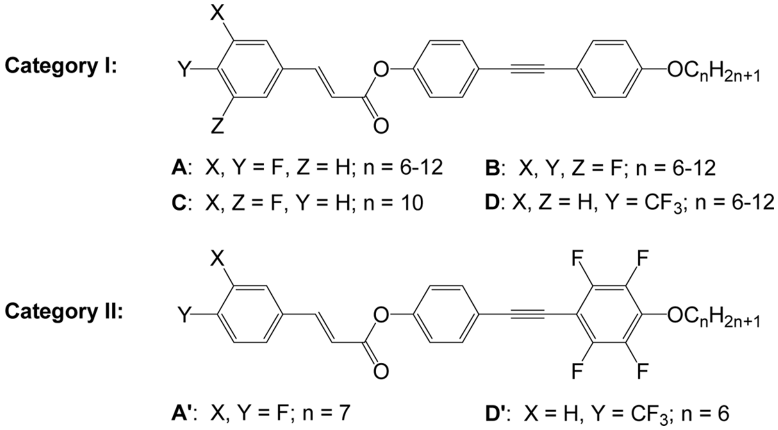

Scheme 1. Chemical structures of the target compounds.

ester moieties to further explore the structure-property relationships of tolane-based LCs (Scheme 1). The role of the trans-double bond can be revealed by comparing with reported tolane benzoates. In addition, the effect of lateral fluorination can be investigated by introducing a 2,3,5,6-tetrafluorophenylene group.

Results and Discussion

The synthesis of the target fluorinated liquid-crystal series are summarized in Scheme 2. Fluorinated benzaldehydes **1a-c** were prepared by formylation of polyfluorophenyl Grignard reagents, and 4-trifluoromethylbenzaldehyde (**1d**) was

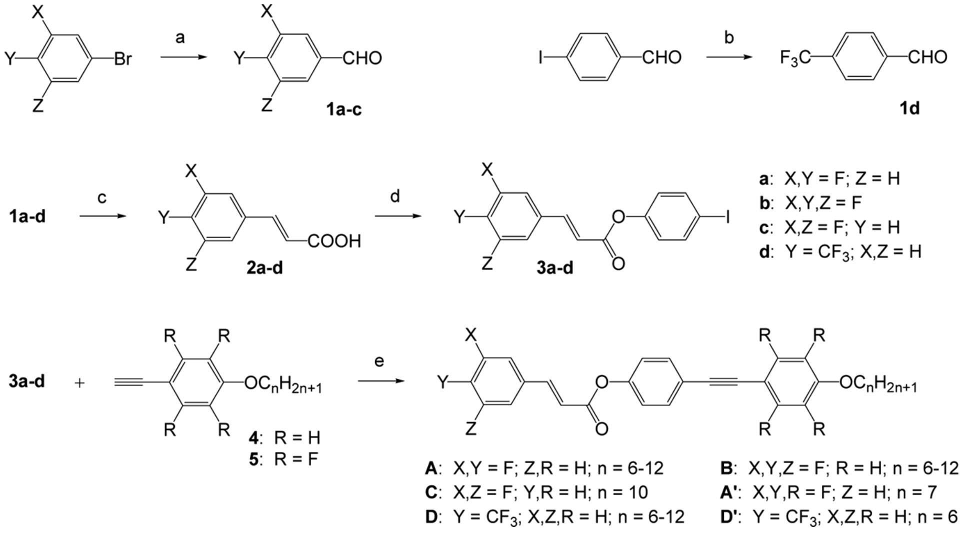

Scheme 2. Synthesis of target compounds: (a) 1, Mg, THF; 2, DMF; (b) $FSO_2CF_2CO_2CH_3$, CuI, DMF, 75°C; (c) malonic acid, pyridine, piperidine, reflux; (d) 4-iodophenol, DCC, cat. DMAP, CH_2Cl_2; (e) cat. $Pd(PPh_3)_2Cl_2$, CuI, Et_3N, reflux.

obtained from 4-iodobenzaldehyde by a copper-catalyzed trifluoromethylation using methyl 2,2-difluoro-2-(fluorosulfonyl)acetate ($FSO_2CF_2CO_2CH_3$) [17]. Benzaldehydes **1a-d** were then converted to cinnamic acids **2a-d** through reactions with malonic acid in pyridine and piperidine. *N*,*N*-Dicyclohexylcarbodiimide (DCC)-promoted esterifications afforded aryl iodides **3a–d**, which were then reacted with phenyl acetylene **4** or **5** respectively under standard Sonogashira conditions to afford the target compounds.

The phase transition temperatures of series **A**, **A′**, **B**, **C**, **D**, and **D′** are summarized in Table 1. All of the compounds exhibit enantiotropic mesophases in very broad temperature ranges. The compounds show surprisingly high thermal stability. There is no decomposition observed even at 250°C.

The effect of the alkoxy chain length on the mesomorphic properties is visualized with a plot of the transition temperatures as a function of methylene units (n) in the alkyl chain (Figs 1–3). The compounds in series **A** display smectic A and nematic phases on both heating and cooling (Fig. 1). With the length of the alkoxy chain increasing, the clearing points and the temperature ranges of the nematic phase

Table 1. Phase transition temperature of target compounds

Compounds	*n*	Transition temperature (°C)
$\mathbf{A}_{6}$	6	C 122.3 SmA 129.9 N 219.5 I 219.2 N 129.4 SmA 81.4 Recr
$\mathbf{A}_{7}$	7	C 98.1 SmA 158.6 N 214.4 I 214.2 N 157.8 SmA 78.8 Recr
$\mathbf{A}_{8}$	8	C 98.7 SmA 170.9 N 209.7 I 209.4 N 170.5 SmA 72.4 Recr
$\mathbf{A}_{9}$	9	C 103.0 SmA 178.8 N 203.2 I 203.0 N 178.5 SmA 74.6 Recr
$\mathbf{A}_{10}$	10	C 87.2 SmA 182.7 N 198.0 I 197.8 N 182.5 SmA 66.5 Recr
$\mathbf{A}_{12}$	12	C 89.4 SmA 176.7 N 181.7 I 181.5 N 176.5 SmA 73.9 Recr
$\mathbf{A}'_{7}$	7	C 77.5 SmA 146.9 N 184.8 I 184.3 N 146.5 SmA 42.4 Recr
$\mathbf{B}_{6}$	6	C 107.1 SmA 177.9 N 198.7 I 198.5 N 177.5 SmA 78.3 Recr
$\mathbf{B}_{7}$	7	C 105.1 SmA 182.1 N 192.9 I 192.7 N 181.7 SmA 74.1 Recr
$\mathbf{B}_{8}$	8	C 81.9 SmA 185.2 N 190.2 I 190.0 N 184.9 SmA 72.8 Recr
$\mathbf{B}_{9}$	9	C 98.5 SmA 186.5 I 186.4 SmA 69.9 Recr
$\mathbf{B}_{10}$	10	C 81.4 SmA 177.6 I 77.4 SmA 57.2 Recr
$\mathbf{B}_{12}$	12	C 84.6 SmA 183.8 I 183.6 SmA 76.1 Recr
$\mathbf{C}_{10}$	10	C 83.3 SmA 106.3 N 133.0 I 132.6 N 105.6 SmA 82.6 SmC 66.1 Recr
$\mathbf{D}_{6}$	6	C 124.2 SmA 225.6 N 242.5 I 241.6 N 225.4 SmA 120.1 SmB 77.0 Recr
$\mathbf{D}_{7}$	7	C 127.8 SmA 227.2 N 234.8 I 234.5 N 226.7 SmA 119.9 SmB 88.5 Recr
$\mathbf{D}_{8}$	8	C 137.5 SmA 226.2 N 229.9 I 229.6 N 225.8 SmA 118.5 SmB 100.4 Recr
$\mathbf{D}_{9}$	9	C 117.2 SmA 224.8 I 224.5 SmA 116.0 SmB 82.9 Recr
$\mathbf{D}_{10}$	10	C 112.4 SmA 222.0 I 221.5 SmA 118.2 SmB 84.3 Recr
$\mathbf{D}_{12}$	12	C 116.0 SmA 214.5 I 213.9 SmA 115.5 SmB 77.2 Recr
$\mathbf{D}'_{6}$	6	C 76.3 SmA 196.1 N 221.7 I 221.4 N 195.7 SmA 37.3 Recr

Cr = crystal; SmA = smectic A phase; SmB = smectic B phase; SmC = smectic C phase; N = nematic phase; I = isotropic liquid; Recr = recrystal.

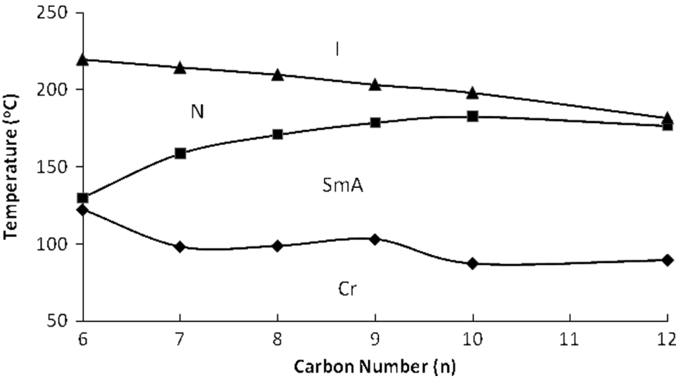

Figure 1. Transition temperatures versus number of methylene units (*n*) of series **A**.

decrease, whereas the ranges of the smectic A phase have an increasing trend because of the increasing lateral interactions; the melting points tend to decrease, but the melting point of compound $\mathbf{A_9}$ is higher than those of compounds $\mathbf{A_8}$ and $\mathbf{A_{10}}$.

Similarly, the clearing points and nematic ranges of series **B** decrease as the chain length increases (Fig. 2). When the alkoxy chain is longer than nine carbons, only a smectic A phase exists. Series **D**, with a trifluoromethyl as the end group, possesses monotropic higher-order smectic B phases besides enantiotropic smectic A and nematic phases (Fig. 3). When $n > 9$, only smectic A and B phases exist. The clearing points also decrease as the length of the alkoxy chain increases.

Comparison between series **A** and reported benzoate analogues **34Fn** [13] shows the effect of the trans-double bond on the liquid-crystalline properties. The clearing points of series **A** and **34Fn** were plotted (Fig. 4) as a function of the length of the alkoxy chain. The clearing points of series **A** are about 20°C–30°C higher than those of the corresponding benzoate analogues. The enhanced mesophase stability of series **A** is attributed to the longer conjugated system when a trans-double bond is added into the rigid liquid-crystalline core. It is worth noting that the introduction of the acrylic ester bridge simplifies the mesomorphic behavior by suppressing the formation of the higher ordered smectic B phase in cooling processes.

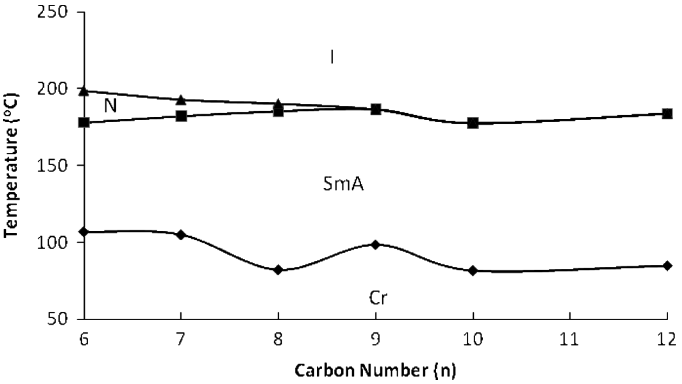

Figure 2. Transition temperatures versus number of methylene units (*n*) of series **B**.

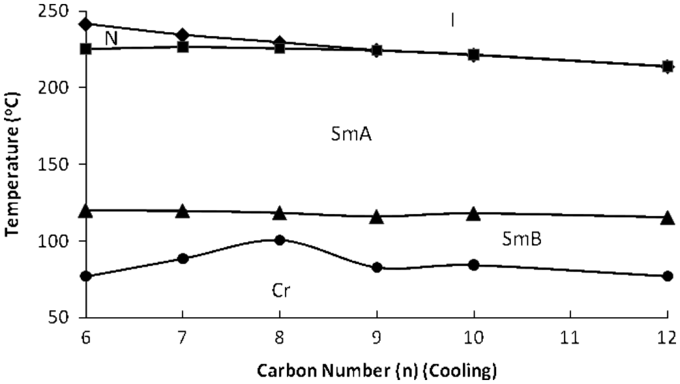

Figure 3. Transition temperatures versus number of methylene units (*n*) of series **D** (cooling).

The clearing points of series **A**, **B**, **D**, and compound $\mathbf{C_{10}}$ as a function of the length of the alkoxy chain are plotted (Fig. 5) in order to study the influence of different fluorination patterns of the end phenyl group on mesomorphic properties. It is found that if the length of alkoxy chains remains the same, the compounds with a 4-trifluoromethylphenyl terminal group (series **D**) have the highest clearing points, and the compounds in series **C**, with a 3,5-difluorophenyl, exhibit the lowest clearing points. The clearing points of 3,4-difluorophenyl-containing series **A** are generally higher than those of 3,4,5-trifluorophenyl-containing series **B**. It is concluded that for different numbers and positions of fluorination, the order of mesophase stability is 4-CF_3- > 3,4-difluoro- > 3,4,5-trifluoro- > 3,5-difluorophenyl. Apparently, a *para*-F or CF_3 group increases both molecular polarity and molecular length and thus raises the clearing points. On the contrary, *meta*-fluorination broadens the molecules, which is unfavorable for formation of liquid-crystalline phases [1].

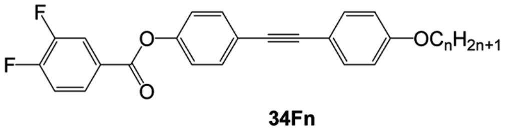

34Fn

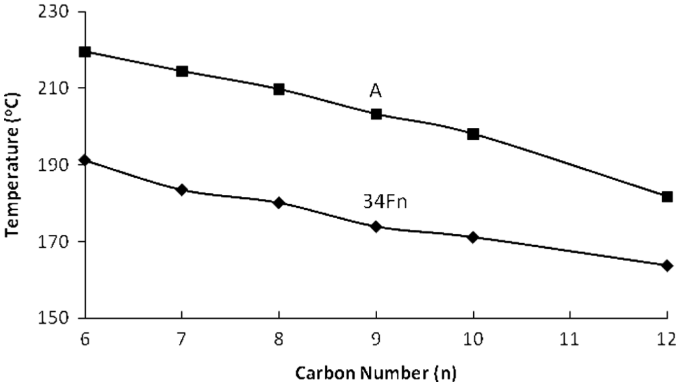

Figure 4. Clearing points versus number of methylene units (*n*) of series **A** and **34Fn**.

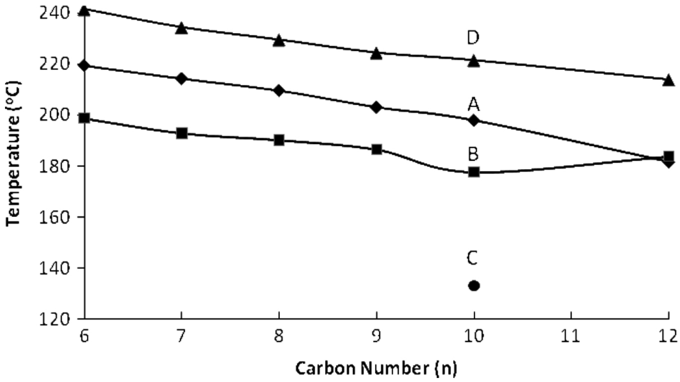

Figure 5. Clearing points versus the number of methylene units (*n*) of series **A**, **B**, **C**, and **D**.

Finally, comparing $\mathbf{A_7}$ with $\mathbf{A'_7}$ and $\mathbf{D_6}$ with $\mathbf{D'_6}$ reveals the effect of lateral fluorination. The introduction of 2,3,5,6-tetrafluorophenylene moiety decreases both the melting and clearing points. Suppressing formation of monotropic smectic B phase is also observed ($\mathbf{D_6}$ versus $\mathbf{D'_6}$). This is consistent with reported results on other systems [18].

Conclusion

In summary, two categories of cinnamate tolane-type LCs were synthesized and their mesomorphic properties were characterized. The compounds generally exhibit smectic A and nematic phases over wide temperature ranges. The effects of the alkoxy chain length, the introduction of the trans-double bond and that of 2,3,5,6-tetrafluorophenylene, and the fluorination patterns of the end phenyl group on mesomorphic properties were investigated. The introduction of acrylate linkers increases the clearing points by 20°C–30°C and suppresses the formation of higher ordered monotropic smectic B phases. *para*-Fluorination is favorable for the mesophase stability, whereas *meta*-fluorination is not. The introduction of 2,3,5,6-tetrafluorophenylene decreases the clearing points and also suppresses the formation of the monotropic smectic B phase.

Experimental

Characterization

The structures of the intermediates and the target compounds were verified by spectrometric methods. Infrared (IR) spectra were recorded on a Perkin Elmer IR-983 spectrophotometer. Nuclear magnetic resonance (NMR) spectra were recorded on a Bruker Advance-300 spectrometer (300 MHz), Varian EM 360 L spectrometer (60 MHz), or a JEOL FX-90Q NMR (90 MHz) with tetramethylsilane (TMS) as internal standard for^{1}H-NMR and trifluoroacetic acid (TFA) as external standard for ^{19}F-NMR. The high field was set to be positive in ^{19}F-NMR spectra. Mass spectra were obtained with a Finnigan 4021 mass spectrometer using electrical ionization. High-resolution mass spectra were recorded with Kratos Concept 1H mass spectrometer.

The transition temperatures of the final liquid-crystalline compounds were measured by a polarizing optical microscope (Olympus PM-6) fitted with a heating stage (Mettler FP-80) and a control unit (FP-82) and also by a differential scanning calorimeter (Shimadzu DSC-50) with heating/cooling rate 5°C/min. The transition temperatures in this article are the peak values of the transitions on DSC traces. Phase assignment was made by comparing the observed textures with those in the literature [19–21].

Synthesis

Examples of the typical procedures for the preparation of the intermediates and the target compounds are given as follows: All of the target compounds have satisfying elemental analysis and appropriate ^{1}H- and ^{19}F-NMR, IR, and MS spectra data.

*3,4-Difluorobenzaldehyde (***1a***).* Into a 100 mL dried three-necked round-bottom flask, equipped with a gas inlet and outlet and a dropping funnel, was added magnesium filings (385 mg, 16 mmol), anhydrous tetrahydrofuran (THF; 10 mL), and a small piece of iodine as the initiator. A solution of 3,4-difluorobromobenzene (3.00 g, 15.5 mmol) in anhydrous THF (5 mL) was added dropwise into the flask with stirring. The resulting reaction mixture was stirred at room temperature for 2 h until the magnesium filings disappeared. The obtained Grignard reagent solution was ice-cooled, and a solution of DMF (1.13 g, 15.5 mmol) in anhydrous THF (5 mL) was added. The reaction was stirred at 0°C for 30 min, quenched by adding saturated NH_4Cl solution, and then extracted with diethyl ether. The etheral layer was dried over anhydrous sodium sulfate and was concentrated. The crude product was purified by column chromatography on silica gel (dichloromethane) to give compound **1a** as a colorless liquid (1.53 g, 63%). ^{19}F-NMR ($CDCl_3$/TFA) δ 49.5 (m, 1F), 57.4 (m, 1F).

*4-Trifluoromethylbenzaldehyde (***1d***).* A solution of 4-iodobenzaldehyde (350 mg, 1.5 mmol) in Dimethylformamide (DMF) (5 mL) was added to a mixture of copper (I) iodide (3.00 g, 15.7 mmol), methyl 2,2-difluoro-2-(fluorosulfonyl)acetate (2.59 g, 13.5 mmol), and DMF (20 mL) preheated to 75°C. The reaction was stirred at the same temperature for 10 h, and then cooled down to room temperature and quenched by pouring into water. The mixture was filtered and the filtrate was extracted with diethyl ether. The etheral extract was washed with water, dried over anhydrous sodium sulfate, and concentrated to give a yellow oil (196 mg, yield 75%). ^{1}H-NMR ($CDCl_3$/TMS) δ 7.65 (d, $J = 9.0$ Hz, 2H), 7.90 (d, $J = 9.0$ Hz, 2H), 9.95 (s, 1H). ^{19}F-NMR ($CDCl_3$/TFA) δ −14.0 (s, 3F).

*3-(3,4-Difluoropheny)acrylic acid (***2a***).* 3,4-Difluorobromobenzaldehyde (**1a**) (0.739 g, 5.2 mmol) and malonic acid (1.045 g, 10 mmol) were dissolved in pyridine (10 ml) in a 50-ml dried 3-necked round bottom flask. Piperidine (0.5 ml) was added in one portion. The resulting mixture was stirred at 85°C for 25 hours, and then refluxed for 3 hours. After cooling down to room temperature, the solution was acidified by adding 10 M hydrochloric acid (7 ml), and extracted twice with diethyl ether. The combined ethereal extracts were washed with water, dried over anhydrous sodium sulfate, and concentrated to give the title compound as a light-pink solid (710 mg, yield 74%). ^{1}H-NMR ($CDCl_3$/TMS) δ 6.50 (d, $J = 16.0$ Hz, 1H), 7.65 (d, $J = 16.0$ Hz, 1H), 7.50 (m, 3H). ^{19}F-NMR ($CDCl_3$/TFA) δ 61.5 (m, 1F), 63.5 (m, 1F).

*3-(3,4-Difluoropheny)acrylic acid 4-iodophenyl ester (***3a***).* Compound **2a** (580 mg, 3.15 mmol) and 4-iodophenol (763 mg, 3.46 mmol) were stirred with DCC (721 mg, 3.5 mmol) and 4-Dimethylaminopyridine (DMAP) (20 mg) in dichloromethane (20 mL) in a single-necked round-bottom flask for 10 h. The resulting slurry was filtered and the filtrate was concentrated. The solid residue was purified by column chromatography on silica gel with petroleum ether/ethyl acetate (5:1) as the eluent to give a white solid (1.12 g, yield 92%). ^{1}H-NMR ($CDCl_3$/TMS) δ 6.45 (d, $J = 16.0$ Hz, 1H), 7.65 (d, $J = 16.0$ Hz, 1H), 6.90 (d, $J = 9.0$ Hz, 2H), 7.65 (d, $J = 9.0$ Hz, 2H), 7.30 (m, 3H). ^{19}F-NMR ($CDCl_3$/TFA) δ 55.0 (m, 2F), 58.0 (m, 1F). MS (m/z, %): 386 (M^+, 8.58).

3-(3,4-Difluorophenyl)acrylic acid 4-(4-decyloxyphenylethynyl)phenyl ester (A_{10}, $n = 10$). A mixture of compound **3a** (120 mg, 0.31 mmol), compound **4** ($n = 10$); (80 mg, 0.31 mmol), bis(triphenylphosphine)palladium dichloride (15 mg), copper (I) iodide (5 mg), and anhydrous triethylamine (15 mL) was stirred under reflux for 3 h under nitrogen protection. After the reaction was completed, the mixture was cooled to room temperature, diluted with diethyl ether, and filtered to remove the precipitates. The filtrate was washed with water, dried over anhydrous sodium sulfate, and concentrated. The pure product was obtained by column chromatography on silica gel (petroleum ether/ethyl acetate 10:1) followed by recrystallization from methanol-acetone to give compound $\mathbf{A_{10}}$ as white crystals (72 mg, yield 45%). ^{1}H-NMR ($CDCl_3$/TMS) δ 0.90 (t, $J = 6.0$ Hz, 3H), 1.10–1.90 (m, 16H), 4.00 (t, $J = 6.0$ Hz, 2H), 6.50 (d, $J = 16.0$ Hz, 1H), 7.75 (d, $J = 16.0$ Hz, 1H), 6.85 (d, $J = 8.0$ Hz, 2H), 7.25 (d, $J = 8.0$ Hz, 2H), 7.13 (d, $J = 8.0$ Hz, 2H), 7.55 (d, $J = 8.0$ Hz, 2H), 7.40 (m, 3H). ^{19}F-NMR ($CDCl_3$/TFA) δ 55.30 (m, 1F), 58.30 (m, 1F). IR (KBr, cm^{-1}) 2955, 2920, 2851, 2219, 1735, 1725, 1641, 1605, 1513, 1281, 1204, 1169, 1020, 840, 776, 529. MS (m/z, %) 516 (M^+, 23.06). HRMS for $C_{33}H_{34}F_2O_3$: Calculated 516.2481; Found 516.2486.

Acknowledgment

This work is supported by the National Natural Science Foundation of China.

References

[1] Hird, M. (2007). *Chem. Soc. Rev.*, *36*, 2070.

[2] Guittard, F., Geribaldi, S., & Cambon, A. (1999). *J. Fluorine Chem.*, *100*, 85.

[3] Gray, G. W., Hird, M., Lacey, D., & Toyne, K. J. (1989). *Mol. Cryst. Liq. Cryst.*, *172*, 165.

[4] Gray, G. W., Hird, M., Lacey, D., & Toyne, K. J. (1991). *Mol. Cryst. Liq. Cryst.*, *195*, 221.

[5] Goulding, M. J., Greenfield, S., Coates, D., & Clemitson, R. (1993). *Liq. Cryst.*, *14*, 1397.

[6] Tsay, K. T., Hsu, C. S., & Wu, S. T. (1998). *Proc. SPIE*, *3421*, 142.

[7] Ichinose, H., Nakajima, S., Sugiyama, Y., Numata, H., Naemura, S., & Manabe, A. (2001). *J. SID*, *9*, 287.

[8] Gauza, S., Wang, H., Wen, C. H., Wu, S. T., Seed, A. J., & Dabrowski, R. (2003). *Jpn. J. Appl. Phys. 1*, *42*, 3463.

[9] Sekine, C., Konya, N., Minai, M., & Fujisawa, K. (2001). *Liq. Cryst.*, *28*, 1495.

[10] Liao, Y. M., Janarthanan, N., Hsu, C. S., Gauza, S., & Wu, S. T. (2006). *Liq. Cryst.*, *33*, 1199.

[11] Xianyu, H. Q., Gauza, S., Song, Q., & Wu, S. T. (2007). *Liq. Cryst.*, *34*, 1473.

[12] Gauza, S., Wen, C. H., Wu, S. T., Janarthanan, N., & Hsu, C. S. (2004). *Jpn. J. Appl. Phys.*, *43*, 7634.

[13] Yang, Y. G., Tang, G., Gong, Z., & Wen, J. X. (2000). *Mol. Cryst. Liq. Cryst.*, *348*, 153.

[14] Yao, L. H., Li, H. F., & Wen, J. X. (2005). *Liq. Cryst.*, *32*, 527.

[15] Chen, X. M., Wang, K., Li, H. F., & Wen, J. X. (2002). *Liq. Cryst.*, *29*, 1105.

[16] Park, J. G., Kim, D. Y., Choi, H. J., & Kim, J. Y. (2001). Cinnamate-containing photopolymer for orientation film of liquid crystal display (LCD) and method for using the photopolymer to form an orientation film. *U.S. Patent 6*, 174,694.

[17] Chen, Q. Y. (1995). *J. Fluorine Chem.*, *72*, 241.

[18] Gray, G. W., Hird, M., Lacey, D., & Toyne, K. J. (1989). *J. Chem. Soc., Perkin Trans. II*, 2041.

[19] Demus, D., & Richter, L. (1979). *Texture of Liquid Crystals*, Verlag Chemie: Weinheim, Germany.

[20] Gray, G. W., & Goodby, J. W. (1986). *Smectic Liquid Crystals: Textures and Structures*, Leonard Hill: Glasgow, UK.

[21] Dierking, I. (2003). *Textures of Liquid Crystals*, Wiley-VCH: Weinheim, Germany.